



Pulmonary Hypertension in Wild Type Mice and Animals with Genetic Deficit in $K_{Ca}2.3$ and $K_{Ca}3.1$ Channels

Christine Wandall-Frostholm^{1*}, Lykke Moran Skaarup^{1*}, Veeranjanyulu Sadda^{1,2}, Gorm Nielsen², Elise Røge Hedegaard¹, Susie Mogensen¹, Ralf Köhler^{2,3}, Ulf Simonsen¹

1 Department of Biomedicine, Aarhus University, Aarhus, Denmark, **2** Institute for Molecular Medicine, Cardiovascular and Renal Research, University of Southern Denmark, Odense, Denmark, **3** Aragon Institute of Health Sciences I+CS and ARAID, Zaragoza, Spain

Abstract

Objective: In vascular biology, endothelial $K_{Ca}2.3$ and $K_{Ca}3.1$ channels contribute to arterial blood pressure regulation by producing membrane hyperpolarization and smooth muscle relaxation. The role of $K_{Ca}2.3$ and $K_{Ca}3.1$ channels in the pulmonary circulation is not fully established. Using mice with genetically encoded deficit of $K_{Ca}2.3$ and $K_{Ca}3.1$ channels, this study investigated the effect of loss of the channels in hypoxia-induced pulmonary hypertension.

Approach and Result: Male wild type and $K_{Ca}3.1^{-/-}/K_{Ca}2.3^{T/T(+DOX)}$ mice were exposed to chronic hypoxia for four weeks to induce pulmonary hypertension. The degree of pulmonary hypertension was evaluated by right ventricular pressure and assessment of right ventricular hypertrophy. Segments of pulmonary arteries were mounted in a wire myograph for functional studies and morphometric studies were performed on lung sections. Chronic hypoxia induced pulmonary hypertension, right ventricular hypertrophy, increased lung weight, and increased hematocrit levels in either genotype. The $K_{Ca}3.1^{-/-}/K_{Ca}2.3^{T/T(+DOX)}$ mice developed structural alterations in the heart with increased right ventricular wall thickness as well as in pulmonary vessels with increased lumen size in partially- and fully-muscularized vessels and decreased wall area, not seen in wild type mice. Exposure to chronic hypoxia up-regulated the gene expression of the $K_{Ca}2.3$ channel by twofold in wild type mice and increased by 2.5-fold the relaxation evoked by the $K_{Ca}2.3$ and $K_{Ca}3.1$ channel activator NS309, whereas the acetylcholine-induced relaxation - sensitive to the combination of $K_{Ca}2.3$ and $K_{Ca}3.1$ channel blockers, apamin and charybdotoxin - was reduced by 2.5-fold in chronic hypoxic mice of either genotype.

Conclusion: Despite the deficits of the $K_{Ca}2.3$ and $K_{Ca}3.1$ channels failed to change hypoxia-induced pulmonary hypertension, the up-regulation of $K_{Ca}2.3$ -gene expression and increased NS309-induced relaxation in wild-type mice point to a novel mechanism to counteract pulmonary hypertension and to a potential therapeutic utility of $K_{Ca}2.3/K_{Ca}3.1$ activators for the treatment of pulmonary hypertension.

Citation: Wandall-Frostholm C, Skaarup LM, Sadda V, Nielsen G, Hedegaard ER, et al. (2014) Pulmonary Hypertension in Wild Type Mice and Animals with Genetic Deficit in $K_{Ca}2.3$ and $K_{Ca}3.1$ Channels. PLoS ONE 9(5): e97687. doi:10.1371/journal.pone.0097687

Editor: Tim Lahm, Indiana University, United States of America

Received: November 7, 2013; **Accepted:** April 22, 2014; **Published:** May 23, 2014

Copyright: © 2014 Wandall-Frostholm et al. This is an open-access article distributed under the terms of the Creative Commons Attribution License, which permits unrestricted use, distribution, and reproduction in any medium, provided the original author and source are credited.

Funding: NovoNordisk Foundation supported Ulf Simonsen and Ralf Köhler. Ulf Simonsen is supported by the Danish Heart Foundation and he is member of LiPhos (Living Photonics: Monitoring light propagation through cells), which is funded by the EC Seventh Framework programme. Ralf Köhler is supported by a grant of the Deutsche Forschungsgemeinschaft (KO1899/11-1) and the Fondo de Investigación Sanitaria (Red HERACLES RD12/0042/0014). The funders had no role in study design, data collection and analysis, decision to publish, or preparation of the manuscript.

Competing Interests: The authors have declared that no competing interests exist.

* E-mail: cwf@farm.au.dk

These authors contributed equally to this work.

Introduction

Pulmonary hypertension is a disabling disease with increased blood pressure in the pulmonary circulation, resulting in shortness of breath, dizziness, edema, right ventricular hypertrophy, heart failure, and premature death. Pulmonary hypertension involves endothelial dysfunction, vasoconstriction, and remodeling of the pulmonary vasculature. The current treatment options are unsatisfactory [1].

The endothelium participates in regulating vascular tone by releasing vasoactive autacoids. Endothelium-dependent relaxation involves the release of a variety of diffusible relaxing factors such as nitric oxide (NO) [2,3], prostacyclin [4], CYP450-generated epoxyeicosanoids acids (11,12-EET and 14,15-EET) [5–7], and an electrical mechanism known as endothelium-derived

hyperpolarization (EDH) [8–10] that produces hyperpolarization of the underlying smooth muscle and closure of voltage-gated calcium channels. The resulting reduction of intracellular calcium leads to relaxation. The small-conductance and intermediate-conductance calcium-activated potassium channels, $K_{Ca}2.3$ and $K_{Ca}3.1$ channel, respectively [11], have been demonstrated to play a significant role in EDH-type relaxation, as a combination of the $K_{Ca}2.3$ and $K_{Ca}3.1$ channel blockers (apamin plus charybdotoxin or apamin plus TRAM-34) inhibits EDH-type relaxation [8,12–14]. Impaired EDH-mediated relaxation involving the $K_{Ca}2.3$ and $K_{Ca}3.1$ channels have been reported to contribute to endothelial dysfunction associated with various human and experimental cardiovascular disease such as hypertension, diabetes, and restenosis [15–18]. In line with the roles of the two channels in endothelial function, $K_{Ca}3.1^{-/-}$ mice have been reported to have

moderately elevated blood pressure [19] and to develop mild left ventricular hypertrophy, as well as a pronounced defect of endothelium-dependent acetylcholine-induced relaxation in both carotid artery and resistance vessels [19,20]. Likewise, suppression of $K_{Ca2.3}$ gene expression in $K_{Ca2.3}^{T/T(+DOX)}$ mice has been shown to elevate blood pressure and increase pressure- and phenylephrine-induced constrictions [21]. Combined $K_{Ca3.1}$ - and $K_{Ca2.3}$ channel deficiency in transgenic doxycycline-treated $K_{Ca3.1}^{-/-}/K_{Ca2.3}^{T/T(+DOX)}$ mice has been reported to increase blood pressure, reduce hyperpolarization of endothelial cells, and to reduce acetylcholine-induced relaxation in carotid arteries and resistance arteries, although the combined deficiency of the two channels has no additive effects on blood pressure [22]. While the roles of the $K_{Ca2.3}$ - and the $K_{Ca3.1}$ channels have been at least partially elucidated for systemic blood pressure control [19,21–23], the precise role of the channels in the pulmonary circulation is still unclear.

Thus far, $K_{Ca2.3}$ and $K_{Ca3.1}$ expression have been found in human, porcine, and rat pulmonary artery endothelial cells [24–27], as well as in the bronchial epithelium [26,27]. In pulmonary arteries relaxation sensitive to blockers of the $K_{Ca2.3}$ and $K_{Ca3.1}$ channels has been observed in several studies [26,28–30]. Moreover, the potent $K_{Ca2.3}$ - and $K_{Ca3.1}$ channel activator NS309 (6,7-dichloro-1H-indole-2,3-dione 3-oxime) has been shown to induce relaxation being sensitive to $K_{Ca2.3}$ - and $K_{Ca3.1}$ blockade in rat and human pulmonary arteries [26,27], rat mesenteric arteries [31], and in porcine retinal arterioles [32]. In addition, $K_{Ca3.1}$ expression has also been found in proliferating vascular smooth muscle cells [33,34], and it may also be increased in the smooth muscle of the hypertrophied arteries in pulmonary hypertension.

In this study, we used $K_{Ca3.1}^{-/-}/K_{Ca2.3}^{T/T(+DOX)}$ mice to study the physiological role of $K_{Ca2.3}$ and $K_{Ca3.1}$ channels in the pulmonary arteries from mice with hypoxia-induced pulmonary hypertension. Our hypothesis was that $K_{Ca2.3}$ and $K_{Ca3.1}$ channels participate in maintaining endothelial function in the pulmonary vasculature, whereas deficiency of $K_{Ca2.3}$ - and $K_{Ca3.1}$ channels aggravates endothelial dysfunction, and thereby contributes to pulmonary hypertension and the associated structural pathologies. Moreover, we tested whether activation of the channels by NS309 improves endothelium-dependent vasodilatation in pulmonary arteries of mice with hypoxia-induced pulmonary hypertension.

Materials and Methods

Ethics statement

This study followed the recommendations in the Guide for the Care and Use of Laboratory Animals of the National Institutes of Health and the ARRIVE Guidelines. The animal studies were approved by the Animal Ethical Committee according to Danish legislation (permit no. 2011/561-2011).

Animal model

The mice were housed in standard cages and had free access to water and food. $K_{Ca3.1}^{-/-}/K_{Ca2.3}^{T/T}$ mice were generated by interbreeding of $K_{Ca3.1}^{-/-}$ [19] and $K_{Ca2.3}^{T/T}$ [35] mice as previously described [22]. 32 Male C57Bl/6 mice and $K_{Ca3.1}^{-/-}/K_{Ca2.3}^{T/T}$ mice, with an age between 15–25 weeks, were given doxycycline (DOX) (Piggidox, 2 mg/kg) in the drinking water, six days before the start of the experiment and throughout the experiment for the suppression of the $K_{Ca2.3}$ channel in the $K_{Ca3.1}^{-/-}/K_{Ca2.3}^{T/T}$ mice. Each genotype was divided into normoxic and hypoxic groups. The hypoxic groups were placed

in hypobaric chambers and exposed to hypoxia for four weeks to induce pulmonary hypertension. The hypobaric chambers were connected to a vacuum pump and depressurized to 560 mbar corresponding to an atmospheric oxygen tension of 10%, as previously described for rats [36].

Hemodynamic measurements

The animal was weighed and anaesthetized by an intraperitoneal injection with a combination of fentanyl (3.313 mg/kg), fluanisone (104.8 mg/kg), and midazolam (52.44 mg/kg), and if necessary the anesthesia was maintained every 30 min. The neck area was shaved and the animal was placed on a heating pad. A 1 cm incision was made on the right side of the neck. By blunt dissection, the right external jugular vein was located and isolated. A hole was cut in the vein and through this, a catheter (SPC-1000, Millar Instruments Inc, USA) was inserted and secured by a suture. The catheter was led into the right ventricle and the position was confirmed by observing the characteristic ventricular waveform. The pressure profile was recorded over a three minute period using a Quad Bridge amplifier connected to a PowerLab device (ADInstruments, Oxfordshire, England) and recorded with Chart 5.5 (ADInstruments). The animal was euthanized after blood pressure measurement by cervical dislocation.

Assessment of right ventricular hypertrophy

Immediately after the mice were sacrificed, heart, lungs, and liver were removed and kept in cold (5° C) physiological saline solution (PSS). A blood sample was collected in a microcapillary tube and centrifuged (International equipment company, microcapillary centrifuge model M B) for three hours as previously described [36].

The hematocrit value was calculated as the length of the erythrocyte layer divided by the length of the entire blood sample. Wet weight of liver and left lung were determined and expressed as percentage of body weight. The heart was isolated and both atria were removed. The free wall of the right ventricle (RV) was separated from left ventricle and septum (LV+S). Each part was weighed and the ratios of right ventricle to left ventricle plus septum (RV/(LV+S)) were calculated and used to assess right ventricular hypertrophy. The thickness of the right ventricular free wall, as well as the septum was measured with a Zeiss Eyepiece calibrating reticule at three different points, at the middle of the wall, and each half then bisected in a cranial and caudal direction, respectively.

QPCR

Samples of lung tissue were dissected and placed in RNAlater filled Eppendorff tubes at 4°C for 24 hours and then stored at –20°C. RNA was extracted using Trizol reagent (Invitrogen, Naerum, Denmark), and genomic DNA was eliminated using DNase I (Qiagen Germantown, MD). The concentration of RNA was determined densitometrically at 260 nm. Reverse transcription of RNA was performed using iScript cDNA synthesis kit (Bio-Rad, Copenhagen, Denmark). A standard PCR protocol was used with initial denaturing at 95°C for 3 min and subsequently 40 cycles of denaturing at 95°C for 25 sec, annealing at 57°C for 20 sec and extending at 72°C for 40 sec. A final step of extension was done at 72°C for 3 min. The PCR-products were analyzed by gel electrophoresis using 1.5% agarose in Tris-borate-EDTA buffer and staining with GelRed™ (Biotium, Hayward, CA). Semiquantitative RT-PCR was done using iQ™ CYBR® Green Supermix (Bio-Rad) and a Stratagene MX3000p cyler (Stratagene, La Jolla, CA) with an initial denaturing at 95°C for 10 min followed by 40 cycles of denaturing at 95°C for 20 sec, annealing at 60°C for 20

sec and an extension step at 72°C for 20 sec. Thereafter, a three-step series of 95°C for 60 sec, 55°C for 30 sec, and a gradual increase to 95°C was run to determine melting points of qPCR products. Signals were normalized to expression of the house keeping gene clathrin (CLCT) and are given as % CLCT. The identity of all PCR products was verified by sequencing. Specific RT-PCR primers were designed to span intronic sequences. The expected product lengths were 226 bp for K_{Ca}2.1, 250 bp for K_{Ca}2.2, 70 bp for K_{Ca}2.3, 217 bp for K_{Ca}3.1, 349 for K_{Ca}1.1, 416 bp for endothelial nitric oxide synthase (eNOS), 152 bp for smooth muscle actin (SMA), 176 bp for collagen-1, and 150 bp for transforming growth factor β (TGFβ). Primer sequences were as follows (5' → 3'): K_{Ca}2.1 FP, TCAAAAATGCTGCTGCAAAAC; K_{Ca}2.1 RP, TCATATGCGATGCTCTGGTGC; K_{Ca}2.2 FP, GGTCATTGAGACCGAGCTGT; K_{Ca}2.2 RP, ATTCCCAGG-TATGGGATGGA; K_{Ca}2.3 FP, CCATGCCAAAGTCAGGAA-AC; K_{Ca}2.3 RP, CATCTTGACACCCGAGT; K_{Ca}3.1 FP, CTGAGAGGCAGGCTGTCAATG; K_{Ca}3.1 RP, ACGTGT-TCTCCGCTTGT; K_{Ca}1.1 FP, ACACTTGACGCCTC-TTATC; K_{Ca}1.1 RP, CTCTGGCAAGATCATGTGGA; eNOS FP, GGTGTCCCTAGACACGA; eNOS RP, CTCGAAAG-CCTCCTCT; SMA FP, AATGGCTCTGGGCTCTGTAA; SMA RP, CTCTTGCTCTGGGCTTCATC; Collagen-1 FP, GAACCCCAAGGAAAAGAAGC; Collagen-1 RP, GCTACGC-TGTTCTTGCACTG; TGFβ FP, ACCGAGAGCCCTGGA-TAC; TGFβ RP, AGGGTCCCAGACAGAAGTTG; CLCT FP, AAGGAGGCGAAACTC ACAGA; CLCT RP, GAGCAGTCA ACATCCAGCAA.

In previous studies we have performed immunoblotting of lungs from rat and man [26,27], but unfortunately we were unable to validate the gene expression results in this study with protein quantification in mouse lung using western blotting, as we experienced a series of difficulties (e.g. lack of specificity and multiple bands) with the mouse antibodies for the K_{Ca}2.3 and K_{Ca}3.1 channels, despite trying several types (K_{Ca}2.3: SC-28621 (Santa Cruz Biotechnology, Santa Cruz, CA); APC-025 (Alamone Labs, Jerusalem, Israel); H00003782-A01 (Abnova, Taiwan). K_{Ca}3.1: P4997, AV35098 (Sigma-Aldrich, St. Louis, MO); SC-32949 (Santa Cruz Biotechnology); CA1788 (Cell Applications, San Diego, CA). All mice were genotyped and QPCR performed as stated above.

Genotyping

All animals were tested for the presence of the K_{Ca}3.1^{-/-} and K_{Ca}2.3^{T/T} alleles by polymerase chain reaction (PCR) on DNA extracts from tail tips. The reaction was carried out in a thermal cycler (ABI system, Applied Biosystems, Carlsbad, CA) using the following protocol, an initial denaturation step at 94°C for 3 min, followed by 10 cycles consisting of 35 sec at 94°C, 35 sec at 58°C and 50 sec at 72°C, proceeded by 25 cycles of the same three steps at the same temperature but with additional 5 sec prolongation at the extension step per cycle, and a final extension step (10 min at 72°C). The reaction product was analysed on a 1% agarose gel. The primer sequence were as follows K_{Ca}2.3^{T/T}: Forward primer (FP) 5'-ATGGACACTTCTGGGCACTT-3', Reverse Primer (RP) 5'-AGAGTGCAACAGACCAGGAT; K_{Ca}3.1^{+/+}/K_{Ca}3.1^{-/-}: FP 5'-CTTTGGATCCAGATGTTTCTTGGTG- 3', K_{Ca}3.1^{+/+} RP 5'-GCCACAGTGTGTCTGTGAGG-3'; K_{Ca}3.1^{-/-} RP 5'-CGT-GCAATCCATCTTGTTC-3'.

Lung perfusion and immunohistochemistry

Catheters with heparin (0.1 ml 100 IU, LEO Pharma, Copenhagen, Denmark) were inserted into the truncus pulmonalis as well as in the trachea and secured by sutures. The left lung lobe was

first perfused with a perfusion mixture (calcium free PSS, 2% albumin, 10% heparin (100 IU), and papaverin (10⁻⁴ M; Sigma-Aldrich)) and then with 4% formaldehyde. The perfusion pressure was maintained at 12–14 mmHg using fluid columns. The left lung lobe was weighed and fixed in 4% formaldehyde for two days and was kept afterwards in ethanol (70%) until embedding in paraffin. The paraffin-embedded left lung lobe was cut in transverse sections of 5 μm. The sections were de-paraffinized and rehydrated by washing 2×5 min each in: xylene, a decreasing ethanol series (99, 96, 76%), and distilled water. Antigen retrieval was performed using a Tris/EDTA pH 9.0 buffer and heating in a microwave for 2×5 min/600 W. Endogenous peroxidase activity was blocked by incubation with 3% H₂O₂ for 20 min, followed by washing for 2×5 min in PBS. To avoid non-specific binding of primary antibodies, sections were incubated with 10% calf serum for 10 min. Thereafter, sections were incubated at 4°C overnight with anti-Von Willebrand factor (1:500, Dako, Denmark). After washing 2×5 min in PBS, sections were incubated in HRP-conjugated secondary antibody (goat-anti rabbit, 1:3000, Zymed laboratories, USA) for one hour at room temperature and washed again 2×5 min in PBS. DAB chromogen (Sigma, USA) was added and sections were incubated for 5 min. Sections were washed again 4×5 min in PBS and incubated with 10% calf serum for 10 min before incubating with primary anti-α-smooth muscle actin (1:250, Abcam, UK) for 75 min at room temperature. After wash 2×5 min in PBS, sections were incubated in AP-conjugated secondary antibody (donkey-anti goat, 1:500, Abcam, UK) one hour at room temperature and washed again 2×5 min in PBS. Stay red chromogen (Sigma-Aldrich) was added and incubated for 5–10 min. After 5 min wash in distilled water, sections were incubated with Mayer's hematoxylin for 20 sec, washed again in water and mounted using **Fluoromount mounting media** (Sigma-Aldrich).

Morphometric measurements

At 400× magnification small pulmonary vessels of each animal ranging from 10 to 80 μm in internal diameter were counted in a blinded manner. Non-muscular arterioles were detected by the endothelial anti-Von Willebrand staining. To assess the degree of muscularization, the amount of α-SMA-positive vessel wall area was determined. Arteries that contained α-SMA-positive vessel area between 4 and 69% were defined as partially-muscularized. Arteries that contained 70% and above were defined as fully-muscularized. Wall area was expressed as percentage of the vessel using the following formulae: % wall area = ((area_{outer} - area_{inner}) / area_{outer}) × 100. The area was calculated using the two perpendicular diameters for both vessel (diameter_{outer}) and lumen (diameter_{inner}) and applying the area formulae for ellipses (area_{ellipse} = π × the two perpendicular radiuses) to account for deviations from the perfect circle form. To avoid oblique sections, vessels with an area difference of more than 20% between the areal calculated as ellipse and circle (area_{circle} = π × radius²) were excluded.

Functional studies

Segments of 2nd and 3rd order pulmonary artery (approximately 2 mm in length) with an internal diameter of 564±28 μm (n = 55) in wild type mice and of 534±20 μm (n = 58) in K_{Ca}3.1^{-/-}/K_{Ca}2.3^{T/T(+DOX)} mice (n.s. vs. wt) were dissected from the right lung lobes and mounted on two 40 μm wires in microvascular myographs (Danish Myotechnology, Aarhus, Denmark) for isometric tension recordings. The myograph chamber filled with PSS was heated to 37° C and equilibrated with 5% CO₂ in artificial air (20.9% O₂, 74% N₂). The artery segments were

stepwise stretched to 2.4 kPa, corresponding to a transmural pressure of 18 mmHg. The segments were allowed to equilibrate for about 10 min. The viability of the segments was confirmed by their ability to contract to first potassium-rich PSS (KPSS, 60 mM) and subsequently to phenylephrine (PE, 1 μ M). All arteries were incubated with the cyclooxygenase inhibitor indomethacin (3 μ M) for 30 min before concentration-response curves were constructed. One artery segment from each mouse was incubated with the eNOS inhibitor N^G -nitro-L-arginine (L-NNA, 10⁻⁴ M) for 30 min, another segment was incubated with a combination of apamin (5*10⁻⁷ M) and charybdotoxin (ChTx, 10⁻⁷ M) for 15 min, and a third artery segment was kept as a control with no additional inhibitors. The arteries were contracted with PE (10⁻⁷ M) and upon stable contraction, acetylcholine (3*10⁻⁷ M) was added. After a washout and incubation with the respective blockers, the arteries were contracted with PE (10⁻⁷ M) and when stable contraction was obtained, NS309 concentration-response curves (10⁻⁸-3*10⁻⁵ M) were performed. After a washout and incubation with the blockers, the arteries were contracted to PE (10⁻⁷ M) and when the contraction was stable, sodium nitroprusside (SNP) concentration-response curves (10⁻¹⁰-10⁻⁵ M) were performed. The response of the artery segments was measured as the change in force. The data on relaxation are given as percentage (% relaxation) of the contraction induced by PE.

Drugs and solutions

Doxycycline (Piggidox Vet.) was obtained from Boehringer Ingelheim Danmark A/S). Hypnorm (fentanyl citrate 0.315 mg/ml, fluanisone 10 mg/ml) was purchased from VetaPharma Ltd (Leeds, UK) and dormicum (midazolam, 5 mg/ml) from Hoffmann-La Roche (Basel, Switzerland).

For myograph experiments. The PSS was of the following composition (mM): CaCl₂ 1.6, NaCl 119, KCl 4.7, glucose 5.5, MgSO₄ H₂O 1.17, NaHCO₃ 25, KH₂PO₄ 1.18, and EDTA 0.026. The calcium-free PSS solution was of the same composition without CaCl₂ 1.6, and potassium-rich PSS (KPSS) solution was of the same composition with NaCl exchanged with KCl to give a final concentration 60 mM. Acetylcholine, indomethacin, PE; L-NNA, and SNP were purchased from Sigma-Aldrich (St. Louis, MO). Apamin and charybdotoxin were purchased from Latoxan (Valence, France). NS309 was kindly donated from Neurosearch (Ballerup, Denmark). For preparation of stock solutions, all drugs were dissolved in distilled water, with the exception of indomethacin and NS309 that were dissolved in DMSO and further diluted in PSS to achieve the final concentration. Apamin and ChTx were prepared in albumin-coated tubes. All solutions were kept at -20°C until use.

Statistics

The computer program GraphPad Prism (San Diego, CA, USA) was used for statistical analysis. Data were expressed as means \pm SEM and differences between groups were analyzed by using two-way ANOVA followed by Bonferroni post hoc test. A probability value of $P < 0.05$ was considered significant. The data from a vessel was excluded from the dataset due to technical reasons.

Results

Basic characteristics of normoxic and hypoxic strains

Body weight, heart rate, hematocrit, heart weight-, wet lung weight- and liver weight normalized to body weight are presented in Table 1. Age matched $K_{Ca}3.1^{-/-}/K_{Ca}2.3^{T/T(+DOX)}$ mice were smaller than wild type mice. The body weight of chronic hypoxic

mice of either genotype was smaller compared to normoxic mice. Exposure to chronic hypoxia increased hematocrit levels, wet lung weight and liver weight. The chronic hypoxic $K_{Ca}3.1^{-/-}/K_{Ca}2.3^{T/T(+DOX)}$ mice however had a significantly smaller increase in liver weight than the chronic hypoxic wild type mice. The heart weight remained unaltered in the normoxic/chronic hypoxic wild type- and $K_{Ca}3.1^{-/-}/K_{Ca}2.3^{T/T(+DOX)}$ mice.

Hemodynamics

Exposure to chronic hypoxia increased the right ventricular systolic blood pressure in normoxic mice of either genotype by 10 to 12 mm Hg (from 24.3 \pm 1.8 mmHg to 37.4 \pm 1.9 mmHg in wild type mice and from 26.4 \pm 2.6 mmHg to 36.0 \pm 2.4 mmHg in $K_{Ca}3.1^{-/-}/K_{Ca}2.3^{T/T(+DOX)}$ mice) and there were no differences between genotypes (Fig. 1A for means and Fig. 1B for tracings). Heart rate was not affected by chronic hypoxia in either genotype and there were no differences between genotypes (Table 1).

Right ventricular hypertrophy

Right ventricular hypertrophy was assessed by determining the weight ratio of the right ventricle over the left ventricle plus septum (RV/LV+S). The chronic hypoxic mice developed right ventricular hypertrophy compared to normoxic mice (Fig. 1C). There was no difference in the degree of right ventricular hypertrophy between wild type- and $K_{Ca}3.1^{-/-}/K_{Ca}2.3^{T/T(+DOX)}$ mice in hypoxia. However, hypoxic $K_{Ca}3.1^{-/-}/K_{Ca}2.3^{T/T(+DOX)}$ mice had an increased right ventricular wall thickness compared to wild type mice (Fig. 1D).

mRNA expression studies

As shown in Fig. 2A, quantitative RT-PCR confirmed the loss of $K_{Ca}3.1$ -exon 4 transcripts and reduced $K_{Ca}2.3$ mRNA expression in the $K_{Ca}3.1^{-/-}/K_{Ca}2.3^{T/T(+DOX)}$ mice as expected. In wild type mice, exposure to chronic hypoxia up-regulated $K_{Ca}2.3$ and $K_{Ca}1.1$ mRNA expression, whereas $K_{Ca}2.1$ channel expression was down-regulated. With the exception of $K_{Ca}2.3$, mRNA expression of $K_{Ca}1.1$ was also increased in the $K_{Ca}3.1^{-/-}/K_{Ca}2.3^{T/T(+DOX)}$ and $K_{Ca}2.1$ expression was down-regulated in a similar fashion. Neither genotype nor hypoxia affected mRNA expression of $K_{Ca}2.2$ or eNOS.

As shown in Fig. 2B, expression of α -smooth muscle actin (α -SMA) was increased in hypoxic wild type- and $K_{Ca}3.1^{-/-}/K_{Ca}2.3^{T/T(+DOX)}$ mice if compared to the respective normoxic controls. Expression levels of collagen-1 were not altered by hypoxia but were down-regulated in $K_{Ca}3.1^{-/-}/K_{Ca}2.3^{T/T(+DOX)}$ mice compared to wild type mice. TGF β expression was not altered by hypoxia or genotype.

Morphological alterations

The pulmonary vessels were stained for Von Willebrandt factor and α -smooth muscle actin and non-muscularized, partially-muscularized, and muscularized vessels were counted and measured (Fig. 3). Chronic hypoxic mice of either genotype had significantly decreased lumen diameters of non-muscularized vessels when compared to normoxic mice of either genotype (Fig. 4A). In contrast, chronic hypoxia did not alter the lumen diameters of partially-muscularized- or fully-muscularized vessels of either genotype. However, the partially-muscularized as well as the fully-muscularized vessels in $K_{Ca}3.1^{-/-}/K_{Ca}2.3^{T/T(+DOX)}$ mice had larger lumen diameter compared to wild type mice.

As shown in Fig. 4B, the wall/lumen ratio for non-muscularized vessels in $K_{Ca}3.1^{-/-}/K_{Ca}2.3^{T/T(+DOX)}$ mice was significantly different from the wild type mice. There was a tendency towards

Table 1. Characteristics of the animals.

		Wild type	$K_{Ca3.1}^{-/-}/K_{Ca2.3}^{T/T(+DOX)}$
Initial	Normoxia	33±1.68	25±0.61*
body weight (g)	Hypoxia	32±1.35	23±0.65*
End	Normoxia	34±1.11	25±0.77*
body weight (g)	Hypoxia	30±0.76 [#]	21±0.56* [#]
Heart rate	Normoxia	466±33	393±30
(BPM)	Hypoxia	413±48	402±27
Hematocrit	Normoxia	39±3.01	38±3.20
(%)	Hypoxia	54±2.38 [#]	55±3.64 [#]
Heart weight	Normoxia	0.5±0.026	0.5±0.017
(% of BW)	Hypoxia	0.5±0.015	0.5±0.020
RV	Normoxia	0.10±0.003	0.11±0.005
(% of BW)	Hypoxia	0.14±0.006 [#]	0.14±0.006 [#]
LV+S	Normoxia	0.40±0.027	0.39±0.011
(% of BW)	Hypoxia	0.36±0.012	0.36±0.018
Lung weight	Normoxia	0.3±0.047	0.4±0.062
(% of BW)	Hypoxia	0.5±0.059 [#]	0.5±0.063 [#]
Liver weight	Normoxia	4.9±0.69	4.9±0.14
(% of BW)	Hypoxia	6.0±0.21 [#]	5.5±0.16 [#]

Selected morphological and functional characteristics and hematocrit of the normoxic and hypoxic strains. Values are means ±SEM, n = 7–8. BPM = beats per minute. BW = body weight. *P < 0.05 vs. wild type;

[#]P < 0.05 vs. normoxia; 2-way ANOVA (n = 7–8 per group).

doi:10.1371/journal.pone.0097687.t001

an increased wall/lumen ratio in chronic hypoxic wild type mice if compared to normoxic wild type mice, whereas the ratio was lower in chronic hypoxic $K_{Ca3.1}^{-/-}/K_{Ca2.3}^{T/T(+DOX)}$ mice if compared to normoxic $K_{Ca3.1}^{-/-}/K_{Ca2.3}^{T/T(+DOX)}$ mice. The wall/lumen ratio was decreased in partially-muscularized vessels in $K_{Ca3.1}^{-/-}/K_{Ca2.3}^{T/T(+DOX)}$ mice when compared to wild type mice. Exposure to chronic hypoxia reduced the wall/lumen ratio in muscularized vessels of either genotype.

The numbers of partially and fully muscularized vessels were increased in both wild type and $K_{Ca3.1}^{-/-}/K_{Ca2.3}^{T/T(+DOX)}$ mice (Fig. 4C).

For the analysis of wall area, the data were grouped according to vessel lumen categories (lumen diameters (μm): 10–19; 20–29; 60–69; Fig. 4C) as previously described [37]. In the vessels with a lumen from 20–29 μm the wall area was larger in hypoxic than in normoxic wild type mice. In contrast, the wall area of the vessels from $K_{Ca3.1}^{-/-}/K_{Ca2.3}^{T/T(+DOX)}$ mice was unaltered in response to chronic hypoxia. The wall area was less in vessels with lumen diameters of 20–39 μm in lung sections from $K_{Ca3.1}^{-/-}/K_{Ca2.3}^{T/T(+DOX)}$ mice (Fig. 4D).

Functional studies

Precontracted pulmonary arteries from chronic hypoxic wild type mice exhibited significantly impaired acetylcholine-induced (3×10^{-7} M) relaxation if compared to normoxic wild type mice (Fig. 5A). Chronic hypoxia also reduced acetylcholine-induced relaxation in arteries from $K_{Ca3.1}^{-/-}/K_{Ca2.3}^{T/T(+DOX)}$ mice and responses under either conditions were similar to those in the wild type mice (Fig. 5A). The $K_{Ca2.3}$ - and $K_{Ca3.1}$ channel inhibitors, apamin and charybdotoxin reduced the acetylcholine-induced relaxation in both normoxic and chronic hypoxic wild type mice (Fig. 5B). In contrast to wild type mice, apamin and charybdotoxin did not reduce the acetylcholine-induced relaxation in normoxic

$K_{Ca3.1}^{-/-}/K_{Ca2.3}^{T/T(+DOX)}$ mice (Fig. 5B). However, acetylcholine-induced relaxation became sensitive to apamin and charybdotoxin in the hypoxic $K_{Ca3.1}^{-/-}/K_{Ca2.3}^{T/T(+DOX)}$ mice (Fig. 5B, columns on the right). This might be explained by the up-regulation of mRNA expression of $K_{Ca1.1}$ as described above. Inhibition of NO synthesis by L-NNA almost abolished acetylcholine-evoked relaxation in both normoxic and chronic hypoxic wild type mice as well as in $K_{Ca3.1}^{-/-}/K_{Ca2.3}^{T/T(+DOX)}$ mice (Fig. 5C), still suggesting that NO is the major endothelium-derived vasodilator in pulmonary arteries of both strains.

NS309 at 10^{-6} M induced similar relaxations of precontracted pulmonary arteries, in both normoxic and hypoxic wild type mice and $K_{Ca3.1}^{-/-}/K_{Ca2.3}^{T/T(+DOX)}$ mice. However, NS309-evoked relaxations were significantly increased in the chronic hypoxic mice of either genotype (Fig. 5D). Incubation with apamin and charybdotoxin did not significantly reduce NS309-induced relaxations of pulmonary arteries from normoxic wild type and $K_{Ca3.1}^{-/-}/K_{Ca2.3}^{T/T(+DOX)}$ mice (Fig. 5E). However, the larger NS309-induced relaxation in hypoxic wild type mice was significantly reduced by apamin and charybdotoxin (Fig. 5E). In contrast, apamin and charybdotoxin failed to reduce the larger NS309-induced relaxations of pulmonary arteries from $K_{Ca3.1}^{-/-}/K_{Ca2.3}^{T/T(+DOX)}$ mice. This suggested that the larger NS309-induced relaxation observed in pulmonary arteries from hypoxic wild type mice was mediated by $K_{Ca3.1}$ and $K_{Ca2.3}$ channels. L-NNA reduced NS309-evoked relaxations by trend in both wild type and $K_{Ca3.1}^{-/-}/K_{Ca2.3}^{T/T(+DOX)}$ mice and abolished the difference between normoxic and hypoxic mice (Fig. 5F).

Exposure to chronic hypoxia did not alter the concentration-response curve for SNP (Figure S1). These findings suggest that the smooth muscle response to NO was unaltered.

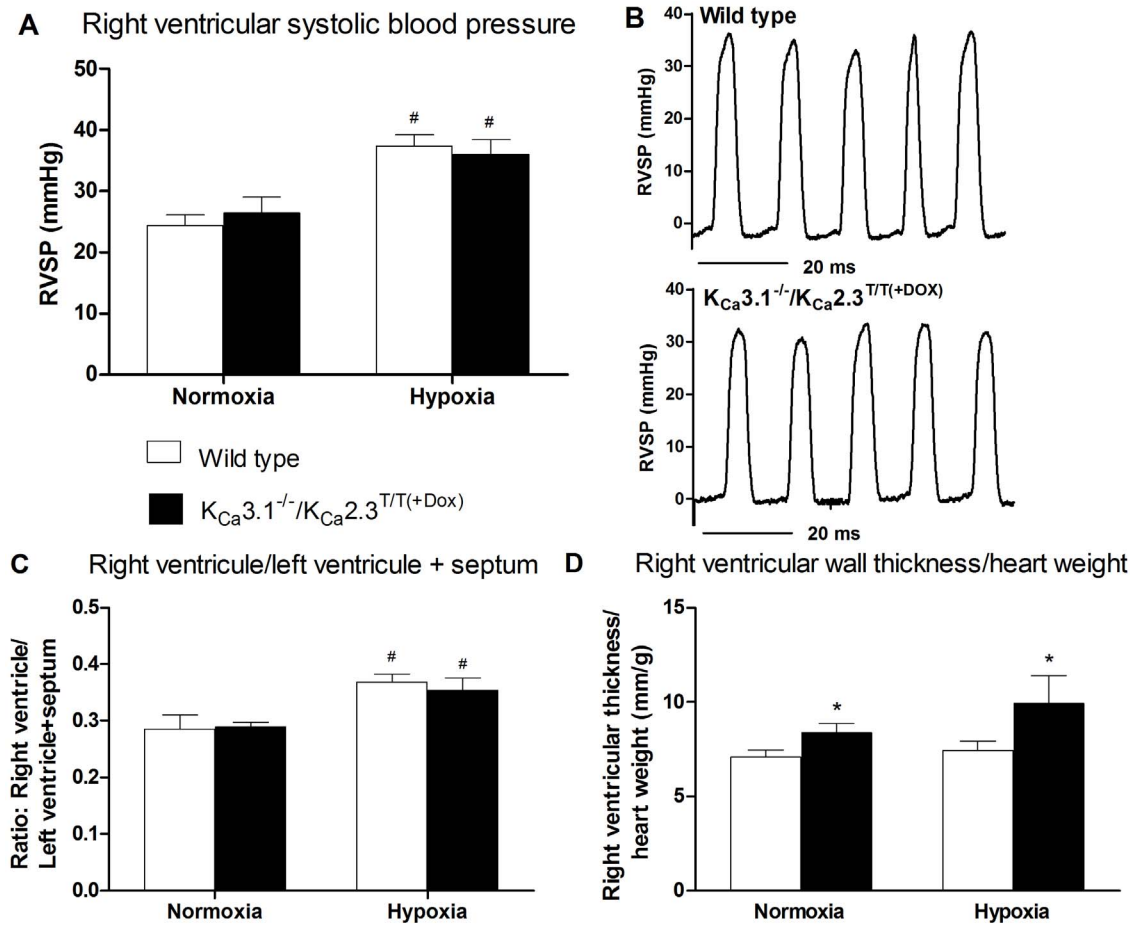


Figure 1. Right ventricular systolic blood pressure and hypertrophy. A) The effect of chronic hypoxia on right ventricular systolic blood pressure (RVSBP) in wild type and $K_{Ca}3.1^{-/-}/K_{Ca}2.3^{T/T(+Dox)}$ mice. Values are means \pm SEM, normoxic wild type ($n=8$) and $K_{Ca}3.1^{-/-}/K_{Ca}2.3^{T/T(+Dox)}$ mice ($n=7$). B) Representative trace of right ventricular pressure measurements in normoxic wild type mice (top) and normoxic $K_{Ca}3.1^{-/-}/K_{Ca}2.3^{T/T(+Dox)}$ mice (bottom). C) Hypoxia induced right ventricular hypertrophy as indicated by alterations of the weight ratio of right ventricle/left ventricle + septum, in wild type and $K_{Ca}3.1^{-/-}/K_{Ca}2.3^{T/T(+Dox)}$ mice, $n=8$. D) The effect of hypoxia on right ventricular wall thickness/heart weight (HW) in wild type and $K_{Ca}3.1^{-/-}/K_{Ca}2.3^{T/T(+Dox)}$ mice. Values are mean \pm SEM, $n=8$. Data were analyzed by 2-way ANOVA and differences were considered significant when $*P<0.05$ vs. wild type, $\# P<0.05$ vs. normoxia. doi:10.1371/journal.pone.0097687.g001

Discussion

The main findings of the present study are that the deficits of the $K_{Ca}2.3$ and $K_{Ca}3.1$ channels failed to change hypoxia-induced pulmonary hypertension, and that chronic hypoxia up-regulated $K_{Ca}2.3$ -gene expression (and also of $K_{Ca}1.1$) and increased NS309-induced relaxation in wild type mice. The latter finding points to a novel mechanism to counteract pulmonary hypertension and implicates a potential therapeutic usage of $K_{Ca}2.3/K_{Ca}3.1$ activators for the treatment of pulmonary hypertension. Moreover, genetic deficit of $K_{Ca}3.1$ channels and partial suppression of $K_{Ca}2.3$ channels caused a significant increase of right ventricular wall thickness and alteration in the pulmonary vessels with reduced wall area of pulmonary vessels and increased lumen diameter in partially-muscularized and fully-muscularized vessels.

The effects of hypoxia-induced pulmonary hypertension in wild type mice

The hypoxic model of pulmonary hypertension mimics the changes in pulmonary circulation seen in high altitude. Mice

exposed to chronic hypoxia develop pulmonary vasoconstriction, pulmonary vascular remodeling, and right ventricular hypertrophy [38].

In this study, the right ventricular systolic blood pressure was significantly increased in the chronic hypoxic mice reflecting pulmonary hypertension. Right ventricular hypertrophy measured as the right ventricle over left ventricle and septum weight ratio, was significantly increased in chronic hypoxic mice, indicating development of pulmonary hypertension in the chronic hypoxic mice.

Our qRT-PCR studies revealed that exposure to chronic hypoxia increased the mRNA expression of $K_{Ca}2.3$ channels by twofold in the lung of wild type mice. Although it appears a limitation of the present study that the increased $K_{Ca}2.3$ expression is found in the lung, it supports our previous studies showing up-regulation of $K_{Ca}2.3$ protein expression in pulmonary arteries without alteration in expression in bronchioles from chronic hypoxic rats [39]. Regarding mRNA expression of $K_{Ca}3.1$ channels in animal models of pulmonary hypertension, previous results have been inhomogeneous: $K_{Ca}3.1$ mRNA expression has been found to be up-regulated in rats with monocrotaline-induced

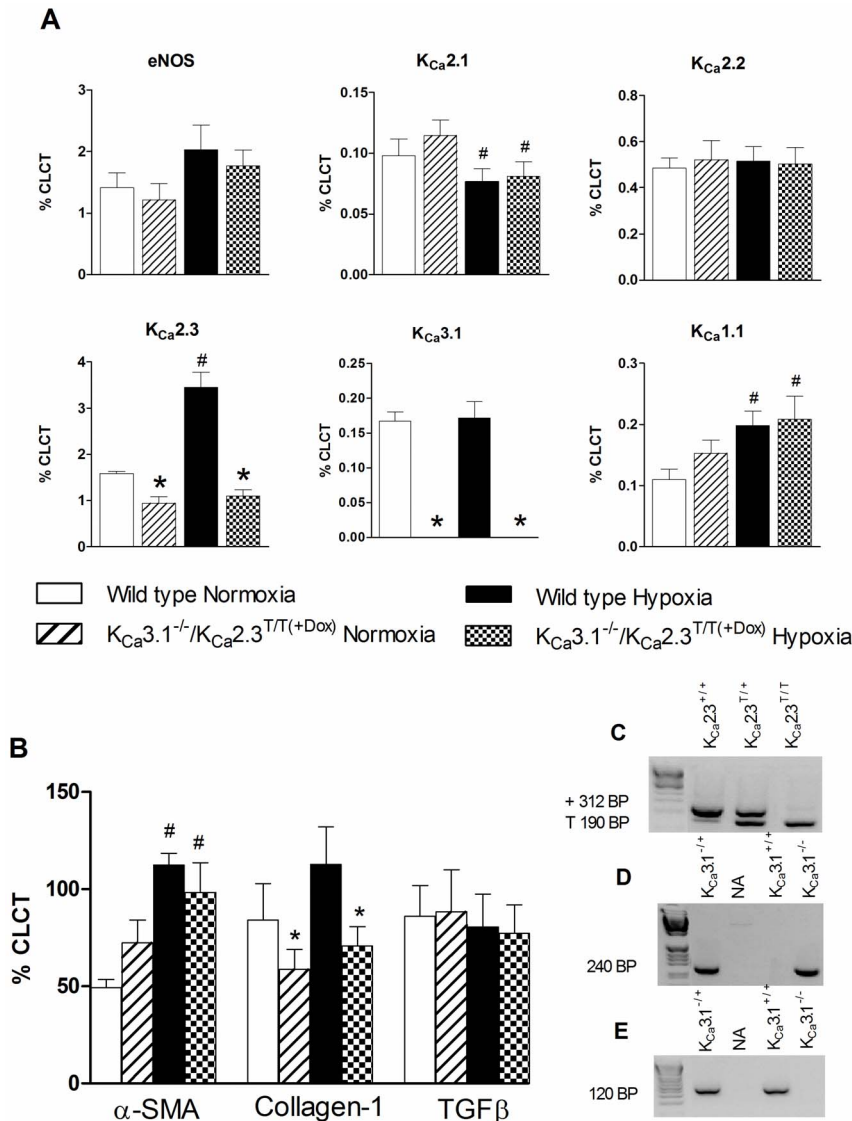


Figure 2. Lung mRNA expression levels of A) eNOS, $K_{Ca}2.1$, $K_{Ca}2.2$, $K_{Ca}2.3$, $K_{Ca}3.1$, and $K_{Ca}1.1$; B) α -Smooth muscle actin (α -SMA), collagen-1, and TGF β . Data are given as means \pm SEM, n=7–8. Data were analyzed by two-way ANOVA and differences were considered significant when * $P < 0.05$ from wild type, # $P < 0.05$ from normoxia. Statistical interaction (ϵ) was observed in $K_{Ca}2.3$ expression (A). C–E) Genotyping: C: Gel electrophoresis shows that polymerase chain reacton (PCR) detected the $K_{Ca}2.3$ -wild type allele (+) and the tTA allele (T) in $K_{Ca}2.3^{T/+}$, and $K_{Ca}2.3^{T/T}$. D and E: PCR detected the targeted allele in $K_{Ca}3.1^{-/+}$ and in $K_{Ca}3.1^{-/-}$ as well as the wild type allele in $K_{Ca}3.1^{-/+}$ and $K_{Ca}3.1^{+/+}$. A DNA ladder was used to determine products sizes.
 doi:10.1371/journal.pone.0097687.g002

pulmonary hypertension [40] or unaltered in chronic hypoxic rats [39]. In the present study on mice, chronic hypoxia did not change the $K_{Ca}3.1$ channel mRNA expression. These discrepancies might be explained by a higher degree of lung fibrosis in monocrotaline-induced pulmonary hypertension than in hypoxia-induced pulmonary hypertension. Development of fibrosis was shown to be accompanied by a higher expression of $K_{Ca}3.1$ [22,41].

Regarding the NO system, a decrease in production or activity of NO was previously found in chronic hypoxic animals. Several studies demonstrated an increase in eNOS mRNA but a decrease in NO activity [42–46], while other studies found that the decreased plasma- and lung perfusate NO_x in piglets was related to a decrease in eNOS mRNA rather than decreased activity [47]. In this study, the mRNA expression of eNOS was not significantly

changed in the hypoxic mice albeit NO-mediated relaxation of pulmonary arteries in chronically hypoxic mice was reduced as detailed below. This indicates endothelial dysfunction at the level of NO activity and in the absence of compensatory up-regulation of eNOS-mRNA expression.

Hypoxia-induced pulmonary hypertension is associated with vascular remodeling in pulmonary arteries, including the appearance of smooth muscle-like cells in previously non-muscularized vessels, thickening of the media and increased accumulation of smooth muscle cells as well as increased deposition of extracellular matrix proteins, predominantly collagen and elastin [38]. Here we found increased mRNA levels of α -SMA but not of collagen-1 or TGF β indicating vascular remodeling and media thickening as

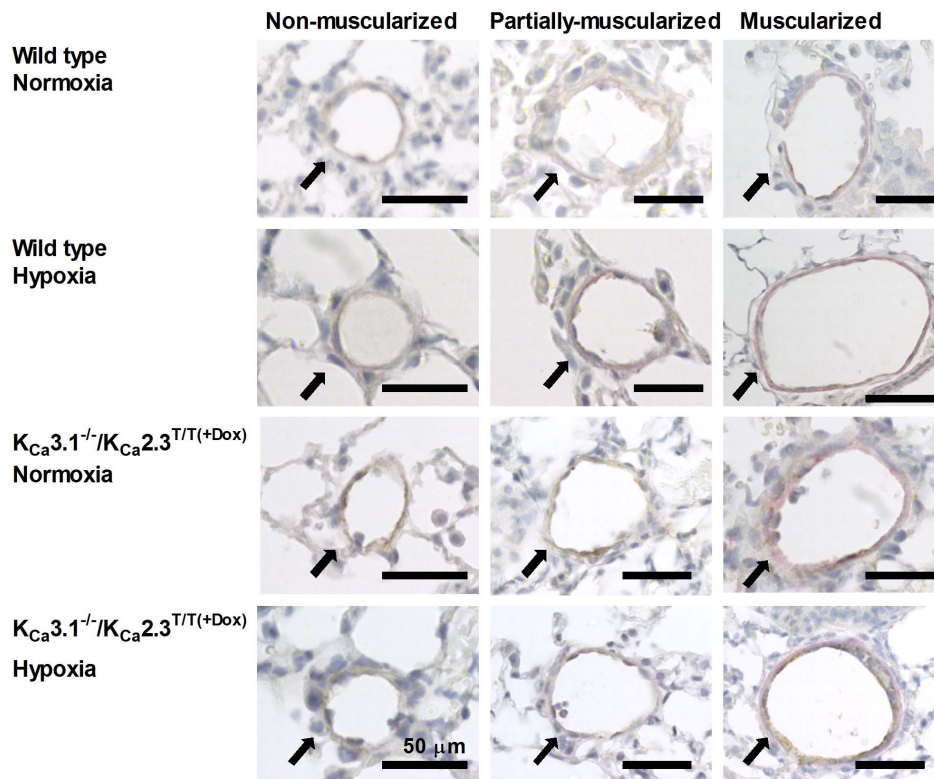


Figure 3. Images of mouse lung showing pulmonary vessels stained for von-Willebrand factor and α -smooth muscle actin from $K_{Ca3.1}^{-/-}/K_{Ca2.3}^{T/T(+Dox)}$ - and wild type mice under normoxic and hypoxic conditions, identifying non-muscularized vessels, partially-muscularized vessels, and fully-muscularized vessels.
doi:10.1371/journal.pone.0097687.g003

outlined above but no substantial pulmonary fibrosis in this murine model.

In agreement with previous studies, exposure to chronic hypoxia and the subsequent development of pulmonary hypertension and of endothelial dysfunction were associated with impaired acetylcholine-induced relaxation in wild type mice [48,49]. The acetylcholine-induced relaxations predominantly involved the NO-pathway as indicated by a full blockade of the response by a blocker of NO-synthesis in hypoxic and normoxic wild type mice. However, also $K_{Ca2.3}$ and $K_{Ca3.1}$ channels contributed to the response in normoxic and hypoxic mice since blockers of the channels clearly reduced the response under either condition.

Regarding the effects of pharmacological activation of the $K_{Ca2.3}$ and $K_{Ca3.1}$ channels in pulmonary arteries, a previous study showed that exposure to chronic hypoxia reduced the relaxations in pulmonary arteries induced by the $K_{Ca3.1}/K_{Ca2.3}$ channel activator NS4591 [39]. In contrast, in our study, chronic hypoxia increased the relaxation to the activator NS309 by 3-fold. This discrepancy might be explained by the 10-fold higher potency of NS4591 on the $K_{Ca3.1}$ channel over the $K_{Ca2.3}$ channel and that in our study NS309 preferentially used the up-regulated $K_{Ca2.3}$ channel expression, as described above, to produce a stronger relaxation. However, NS309 in the present study produced a $K_{Ca2.3}/K_{Ca3.1}$ -independent relaxation. These small dilator effects could be related to the fact that NS309 at concentrations above 10 μ M blocks voltage-dependent Ca^{2+} channels [50] further corroborating substantial unspecific vasodilator effects of this compound. This is further supported by our

observation that the NS309-induced relaxation in normoxic wild type mice was insensitive to the $K_{Ca2.3}$ and $K_{Ca3.1}$ channel blockers, apamin and charybdotoxin, which contrasts with earlier findings in rat arteries [26,39]. Nevertheless, the increased NS309-evoked relaxation in chronic hypoxic mice were sensitive to the $K_{Ca2.3}$ and $K_{Ca3.1}$ channel blockers, suggesting that under these conditions and in keeping with the up-regulation of $K_{Ca2.3}$ in the hypoxic mice, a substantial portion of vasodilator capacity is now carried by activation of the $K_{Ca2.3}$ channel and EDH-vasodilator pathways. This interpretation is further supported by the notion that NS309-induced relaxations were not reduced by L-NNA in these hypoxic mice.

Pulmonary hypertension in mice with genetic deficit of $K_{Ca2.3}$ and $K_{Ca3.1}$ channels

The $K_{Ca3.1}^{-/-}/K_{Ca2.3}^{T/T(+DOX)}$ mice developed increased right ventricular systolic blood pressure as well as increased right ventricular hypertrophy ratio to a similar degree as the hypoxic wild type mice. Furthermore, increased ratios of right ventricular wall thickness/heart weight was found in normoxic and hypoxic $K_{Ca3.1}^{-/-}/K_{Ca2.3}^{T/T(+DOX)}$ mice. This may suggest that the down-regulation of the channels caused hypertrophy of the right heart. In addition, previous studies found that the $K_{Ca2.3}^{T/T}$ mice had structural alterations, including enhancement of arteries and enlargement of other hollow organs [21,51], thus the life-long overexpression of the channel in this genetic model of channel overexpression(-Dox)/suppression(+Dox) may influence cardiac development and morphology.

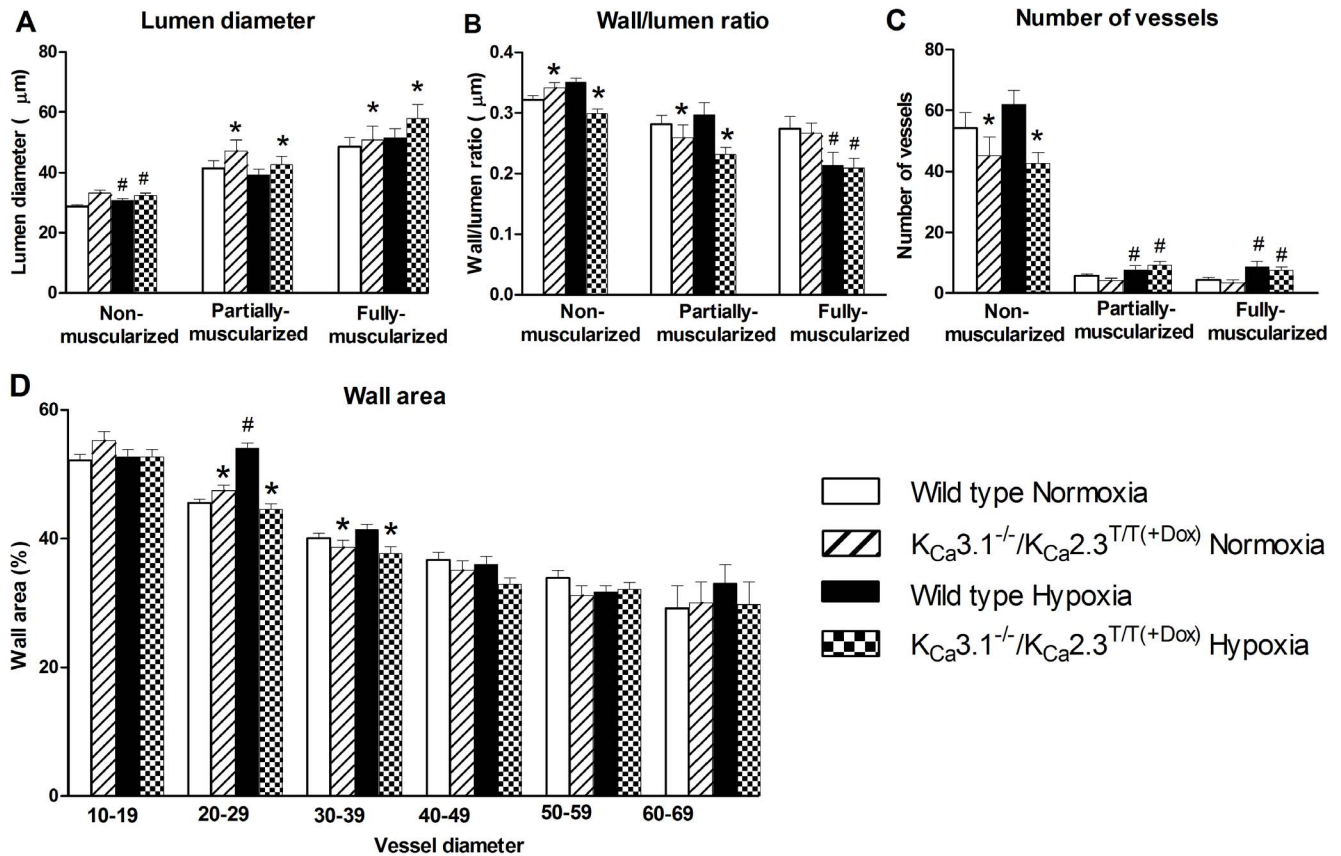


Figure 4. Morphometric measurements. A: Lumen diameter (μm) in vessels divided in groups of non-muscularized-, partially- and fully-muscularized vessels. B: Wall/lumen ratio divided in groups of non-muscularized-, partially- and fully-muscularized vessels. C: Number of non-muscularized-, partially- and muscularized vessels in each experimental group. D: Wall area of the vessels divided in groups of vessel diameter. * $P < 0.05$ vs. wild type and # $P < 0.05$ vs. normoxia. Statistical interaction was observed in Figure (B) for non-muscularized vessels. doi:10.1371/journal.pone.0097687.g004

$K_{Ca}2.3$ mRNA expression was present in Dox-treated $K_{Ca}3.1^{-/-}/K_{Ca}2.3^{T/T}$ mice though expression was significantly lower than in wild types, reflecting the fact that the $K_{Ca}2.3$ channel was suppressed rather than knocked out. $K_{Ca}3.1$ channel expression was almost abolished in $K_{Ca}3.1^{-/-}/K_{Ca}2.3^{T/T(+DOX)}$ mice. It is noteworthy that the genetic alterations did not affect the mRNA expression of the other Ca^{2+} -activated K^{+} channels ($K_{Ca}2.1$, $K_{Ca}2.2$, and $K_{Ca}1.1$) compared to wild type mice and, thus, there was no evident compensation caused by increased channel expression of these related K_{Ca} channels.

Genetic deficit of $K_{Ca}2.3$ and $K_{Ca}3.1$ channels in normoxic and hypoxic $K_{Ca}3.1^{-/-}/K_{Ca}2.3^{T/T(+DOX)}$ mice increased lumen diameter in partially muscularized- and muscularized vessels compared to normoxic and chronic hypoxic wild type mice. This could be due to the structural alterations previously seen in the $K_{Ca}2.3^{T/T}$ mice [21]. Furthermore, the wall area was significantly decreased in $K_{Ca}3.1^{-/-}/K_{Ca}2.3^{T/T(+DOX)}$ mice compared to wild type mice in vessels of 20–39 μm . Intuitively, one would expect that these structural alterations decrease pulmonary pressure. However pulmonary vascular remodeling by itself is not necessarily sufficient for altering pulmonary pressure in chronic hypoxic mice [52]. In the present study the blood pressure was also not altered in the $K_{Ca}3.1^{-/-}/K_{Ca}2.3^{T/T(+DOX)}$ mice compared to wild type mice regardless of normoxic or chronic hypoxic conditions. This can probably be explained by early developmental alterations in this model.

In a previous study, $K_{Ca}3.1^{-/-}$ mice had reduced acetylcholine-induced relaxation in carotid arteries [19]. Similarly, transgenic $K_{Ca}3.1^{-/-}/K_{Ca}2.3^{T/T(+DOX)}$ mice exhibited defective acetylcholine-induced relaxation in carotid- and systemic resistance arteries [22]. Contrary to these previous findings, $K_{Ca}3.1^{-/-}/K_{Ca}2.3^{T/T(+DOX)}$ mice in the present study did not show impaired acetylcholine-induced relaxation in pulmonary arteries compared to wild type mice. However, this might be explained by the fact that the acetylcholine-induced relaxation in the murine pulmonary arteries was almost entirely mediated by NO and insensitive to blockers of $K_{Ca}2.3$ and $K_{Ca}3.1$ channels, while in other vascular beds the $K_{Ca}3.1/K_{Ca}2.3$ -EDH-system and a possible interaction of the EDH with the NO system were found to be more important [22,53].

Surprisingly, exposure to chronic hypoxia converted the acetylcholine-induced relaxation in these mice into an apamin- and charybdotoxin-sensitive relaxation. This could be due to an up-regulation of an apamin-sensitive K^{+} channel and/or a charybdotoxin-sensitive K^{+} channel (such as $K_{Ca}1.1$), as an adaptation to the hypoxic condition in the $K_{Ca}3.1^{-/-}/K_{Ca}2.3^{T/T(+DOX)}$ mice.

In conclusion, chronic hypoxia increased expression of $K_{Ca}2.3$ and $K_{Ca}1.1$ genes, decreased the expression of $K_{Ca}2.1$, and improved the endothelium-dependent vasodilatation to pharmacological activation of the channels. Such a mechanism could be of help to compensate for the loss of NO-activity in pulmonary

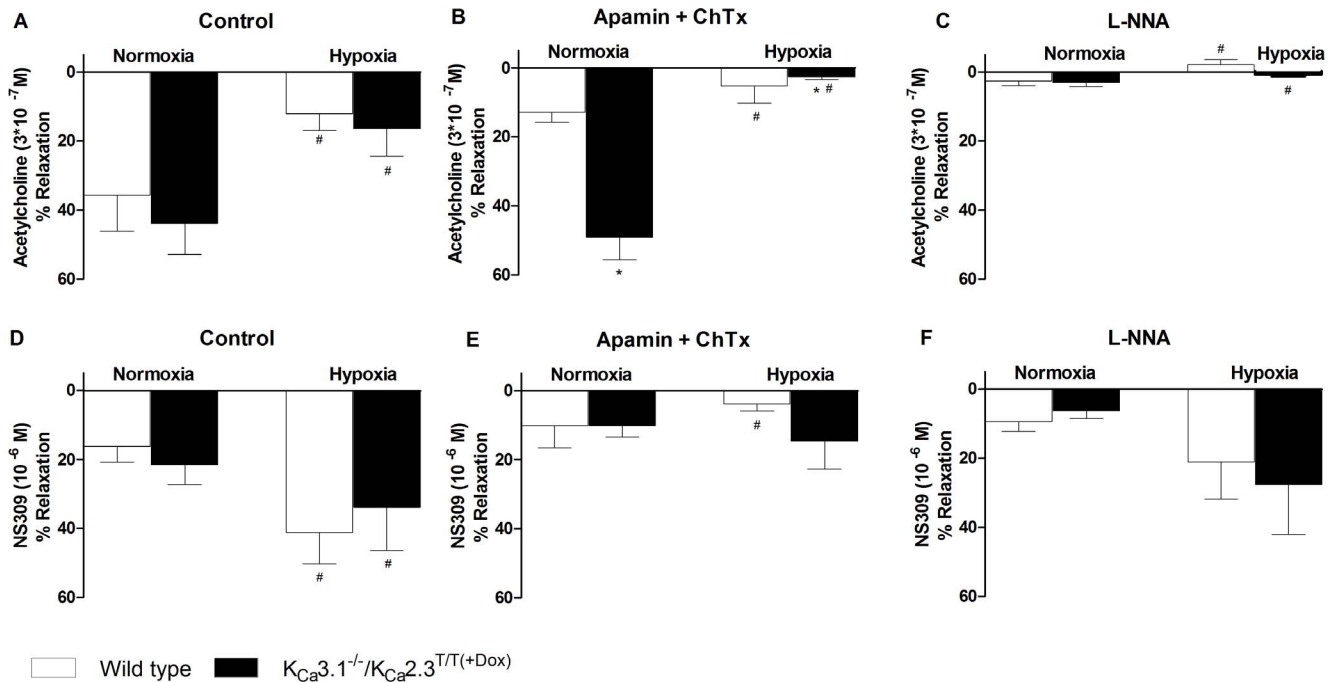


Figure 5. Functional studies of acetylcholine-induced (3×10^{-7} M) relaxation (A–C) and NS309-induced (10^{-6} M) relaxation (D–F) in wild type and $KCa_{3.1}^{-/-}/KCa_{2.3}^{T/T(+Dox)}$ mice. A) Acetylcholine-induced relaxation. B) Acetylcholine-evoked relaxation in the presence of apamin (5×10^{-7} M) and ChTx (10^{-7} M). C) Acetylcholine-evoked relaxation in the presence of L-NNA (10^{-4} M). D) NS309-induced relaxation. E) NS309-induced relaxation in the presence of apamin (5×10^{-7} M) and ChTx (10^{-7} M). F) NS309-evoked relaxation in the presence of L-NNA (10^{-4} M). Data were analyzed by 2-way ANOVA and * $P < 0.05$ vs. wild type and # $P < 0.05$ vs. normoxia; $n = 6-7$ per group. doi:10.1371/journal.pone.0097687.g005

hypertension and could be pharmacologically targeted to counteract pulmonary hypertension. Genetic deficit of $KCa_{3.1}$ and $KCa_{2.3}$ did not worsen pulmonary hypertension or endothelial dysfunction, though it prevented structural vascular remodelling in chronic hypoxia-induced pulmonary hypertension.

Supporting Information

Figure S1 Relaxation to SNP-induced (10^{-10} – 10^{-5} M) in PE (10^{-7} M) pre-contracted arteries, in normoxic wild type and $KCa_{3.1}^{-/-}/KCa_{2.3}^{T/T(+Dox)}$ mice (left) and hypoxic wild type and $KCa_{3.1}^{-/-}/KCa_{2.3}^{T/T(+Dox)}$ mice. (TIF)

References

1. Benza RL, Miller DP, Barst RJ, Badesch DB, Frost AE, et al. (2012) An evaluation of long-term survival from time of diagnosis in pulmonary arterial hypertension from the REVEAL Registry. *Chest* 142: 448–456.
2. Ignarro LJ, Burke TM, Wood KS, Wolin MS, Kadowitz PJ (1984) Association between cyclic GMP accumulation and acetylcholine-elicited relaxation of bovine intrapulmonary artery. *J Pharmacol Exp Ther* 228: 682–690.
3. Palmer RM, Ferrige AG, Moncada S (1987) Nitric oxide release accounts for the biological activity of endothelium-derived relaxing factor. *Nature* 327: 524–526. doi:10.1038/327524a0
4. Moncada S, Vane JR (1978) Pharmacology and endogenous roles of prostaglandin endoperoxides, thromboxane A₂, and prostacyclin. *Pharmacol Rev* 30: 293–331.
5. Campbell WB, Gebremedhin D, Pratt PF, Harder DR (1996) Identification of epoxyeicosatrienoic acids as endothelium-derived hyperpolarizing factors. *Circ Res* 78: 415–423.
6. Fisslthaler B, Popp R, Kiss L, Potente M, Harder DR, et al. (1999) Cytochrome P450 2C is an EDHF synthase in coronary arteries. *Nature* 401: 493–497.
7. Hercule HC, Schunck WH, Gross V, Seringer J, Leung FP, et al. (2009) Interaction between P450 eicosanoids and nitric oxide in the control of arterial tone in mice. *Arterioscler Thromb Vasc Biol* 29: 54–60.
8. Edwards G, Dora KA, Gardener MJ, Garland CJ, Weston AH (1998) K⁺ is an endothelium-derived hyperpolarizing factor in rat arteries. *Nature* 396: 269–272.
9. Busse R, Edwards G, Félétou M, Fleming I, Vanhoutte PM, et al. (2002) EDHF: bringing the concepts together. *Trends Pharmacol Sci* 23: 374–380.
10. Félétou M, Vanhoutte PM (2006) Endothelium-derived hyperpolarizing factor: where are we now? *Arterioscler Thromb Vasc Biol* 26: 1215–1225.
11. Wei AD, Gutman GA, Aldrich R, Chandy KG, Grissmer S, et al. (2005) International Union of Pharmacology. LII. Nomenclature and molecular relationships of calcium-activated potassium channels. *Pharmacol Rev* 57: 463–472.
12. Corriu C, Félétou M, Canet E, Vanhoutte PM (1996) Endothelium-derived factors and hyperpolarization of the carotid artery of the guinea-pig. *Br J Pharmacol* 119: 959–964.
13. Petersson J, Zygmunt PM, Hogestatt ED (1997) Characterization of the potassium channels involved in EDHF-mediated relaxation in cerebral arteries. *Br J Pharmacol* 120: 1344–1350.
14. Yamanaka A, Ishikawa T, Goto K (1998) Characterization of endothelium-dependent relaxation independent of NO and prostaglandins in guinea pig coronary artery. *J Pharmacol Exp Ther* 285: 480–489.

Acknowledgments

We acknowledge laboratory technician Henriette Gram Johanson for excellent technical assistance and Thomas Dalsgaard for helpful discussions.

Author Contributions

Conceived and designed the experiments: CWF ERH RK US. Performed the experiments: CWF LMS VS GN SM. Analyzed the data: CWF LMS VS GN ERH SM RK US. Contributed reagents/materials/analysis tools: RK US. Wrote the paper: CWF RK US. Obtained permission for the animal experiments: US.

15. Grgic I, Kaistha BP, Hoyer J, Köhler R (2009) Endothelial Ca²⁺-activated K⁺ channels in normal and impaired EDHF-dilator responses—relevance to cardiovascular pathologies and drug discovery. *Br J Pharmacol* 157: 509–526.
16. Félétou M (2009) Calcium-activated potassium channels and endothelial dysfunction: therapeutic options? *Br J Pharmacol* 156: 545–562.
17. Köhler R, Kaistha BP, Wulff H (2010) Vascular K_{Ca}-channels as therapeutic targets in hypertension and restenosis disease. *Expert Opin Ther Targets* 14: 143–155.
18. Dalsgaard T, Kroigaard C, Simonsen U (2010) Calcium-activated potassium channels - a therapeutic target for modulating nitric oxide in cardiovascular disease? *Expert Opin Ther Targets* 14: 825–837.
19. Si H, Heyken WT, Wöflle SE, Tysiac M, Schubert R, et al. (2006) Impaired endothelium-derived hyperpolarizing factor-mediated dilations and increased blood pressure in mice deficient of the intermediate-conductance Ca²⁺-activated K⁺ channel. *Circ Res* 99: 537–544.
20. Wöflle SE, Schmidt VJ, Hoyer J, Köhler R, de WC (2009) Prominent role of K_{Ca}3.1 in endothelium-derived hyperpolarizing factor-type dilations and conducted responses in the microcirculation in vivo. *Cardiovasc Res* 82: 476–483.
21. Taylor MS, Bonev AD, Gross TP, Eckman DM, Brayden JE, et al. (2003) Altered expression of small-conductance Ca²⁺-activated K⁺ (SK3) channels modulates arterial tone and blood pressure. *Circ Res* 93: 124–131.
22. Brähler S, Kaistha A, Schmidt VJ, Wöflle SE, Busch C, et al. (2009) Genetic deficit of SK3 and IK1 channels disrupts the endothelium-derived hyperpolarizing factor vasodilator pathway and causes hypertension. *Circulation* 119: 2323–2332.
23. Damkjaer M, Nielsen G, Bodendiek S, Staehr M, Gramsbergen JB, et al. (2012) Pharmacological activation of K_{Ca}3.1/K_{Ca}2.3 channels produces endothelial hyperpolarization and lowers blood pressure in conscious dogs. *Br J Pharmacol* 165: 223–234.
24. Burnham MP, Bychkov R, Félétou M, Richards GR, Vanhoutte PM, et al. (2002) Characterization of an apamin-sensitive small-conductance Ca²⁺-activated K⁺ channel in porcine coronary artery endothelium: relevance to EDHF. *Br J Pharmacol* 135: 1133–1143.
25. Bychkov R, Burnham MP, Richards GR, Edwards G, Weston AH, et al. (2002) Characterization of a charybdotoxin-sensitive intermediate-conductance Ca²⁺-activated K⁺ channel in porcine coronary endothelium: relevance to EDHF. *Br J Pharmacol* 137: 1346–1354.
26. Kroigaard C, Dalsgaard T, Simonsen U (2010) Mechanisms underlying epithelium-dependent relaxation in rat bronchioles: analogy to EDHF-type relaxation in rat pulmonary arteries. *Am J Physiol Lung Cell Mol Physiol* 298: L531–L542.
27. Kroigaard C, Dalsgaard T, Nielsen G, Laursen BE, Pilegaard H, et al. (2012) Activation of endothelial and epithelial K(Ca) 2.3 calcium-activated potassium channels by NS309 relaxes human small pulmonary arteries and bronchioles. *Br J Pharmacol* 167: 37–47.
28. Guérard P, Goirand F, Fichet N, Bernard A, Rochette L, et al. (2004) Arachidonic acid relaxes human pulmonary arteries through K⁺ channels and nitric oxide pathways. *Eur J Pharmacol* 501: 127–135.
29. Fuloria M, Smith TK, Aschner JL (2002) Role of 5,6-epoxyicosatrienoic acid in the regulation of newborn piglet pulmonary vascular tone. *Am J Physiol Lung Cell Mol Physiol* 283: L383–L389.
30. Karamsetty MR, Nakashima JM, Ou L, Klinger JR, Hill NS (2001) EDHF contributes to strain-related differences in pulmonary arterial relaxation in rats. *Am J Physiol Lung Cell Mol Physiol* 280: L458–L464.
31. Stankevicius E, Dalsgaard T, Kroigaard C, Beck L, Boedtker E, et al. (2011) Opening of small and intermediate calcium-activated potassium channels induces relaxation mainly mediated by nitric-oxide release in large arteries and endothelium-derived hyperpolarizing factor in small arteries from rat. *J Pharmacol Exp Ther* 339: 842–850.
32. Dalsgaard T, Kroigaard C, Bek T, Simonsen U (2009) Role of calcium-activated potassium channels with small conductance in bradykinin-induced vasodilation of porcine retinal arterioles. *Invest Ophthalmol Vis Sci* 50: 3819–3825.
33. Neylon CB, Lang RJ, Fu Y, Bobik A, Reinhart PH (1999) Molecular cloning and characterization of the intermediate-conductance Ca²⁺-activated K⁺ channel in vascular smooth muscle: relationship between K(Ca) channel diversity and smooth muscle cell function. *Circ Res* 85: e33–e43.
34. Köhler R, Wulff H, Eichler I, Kneifel M, Neumann D, et al. (2003) Blockade of the intermediate-conductance calcium-activated potassium channel as a new therapeutic strategy for restenosis. *Circulation* 108: 1119–1125.
35. Bond CT, Sprengel R, Bissonnette JM, Kaufmann WA, Pribnow D, et al. (2000) Respiration and parturition affected by conditional overexpression of the Ca²⁺-activated K⁺ channel subunit, SK3. *Science* 289: 1942–1946.
36. Baandrup JD, Markvardsen LH, Peters CD, Schou UK, Jensen JL, et al. (2011) Pressure load: the main factor for altered gene expression in right ventricular hypertrophy in chronic hypoxic rats. *PLoS One* 6: e15859.
37. Cahill E, Costello CM, Rowan SC, Harkin S, Howell K, et al. (2012) Gremlin plays a key role in the pathogenesis of pulmonary hypertension. *Circulation* 125: 920–930.
38. Stenmark KR, Fagan KA, Frid MG (2006) Hypoxia-induced pulmonary vascular remodeling: cellular and molecular mechanisms. *Circ Res* 99: 675–691.
39. Kroigaard C, Kudryavtseva O, Dalsgaard T, Wandall-Frostholm C, Olesen SP, et al. (2013) K_{Ca}3.1 channel downregulation and impaired EDH-type relaxation in pulmonary arteries from chronic hypoxic rats. *Exp Physiol* 98 (4):957–69.
40. Morio Y, Homma N, Takahashi H, Yamamoto A, Nagaoka T, et al. (2007) Activity of endothelium-derived hyperpolarizing factor is augmented in monocrotaline-induced pulmonary hypertension of rat lungs. *J Vasc Res* 44: 325–335.
41. Huang C, Shen S, Ma Q, Chen J, Gill A, et al. (2013) Blockade of K_{Ca}3.1 Ameliorates Renal Fibrosis Through the TGF-beta1/Smad Pathway in Diabetic Mice. *Diabetes* 62: 2923–2934.
42. Shaul PW, North AJ, Brannon TS, Ujici K, Wells LB, et al. (1995) Prolonged in vivo hypoxia enhances nitric oxide synthase type I and type III gene expression in adult rat lung. *Am J Respir Cell Mol Biol* 13: 167–174.
43. Le Cras TD, Xue C, Rengasamy A, Johns RA (1996) Chronic hypoxia upregulates endothelial and inducible NO synthase gene and protein expression in rat lung. *Am J Physiol* 270: L164–L170.
44. Le Cras TD, Tyler RC, Horan MP, Morris KG, Tuder RM, et al. (1998) Effects of chronic hypoxia and altered hemodynamics on endothelial nitric oxide synthase expression in the adult rat lung. *J Clin Invest* 101: 795–801.
45. Xue C, Johns RA (1996) Upregulation of nitric oxide synthase correlates temporally with onset of pulmonary vascular remodeling in the hypoxic rat. *Hypertension* 28: 743–753.
46. Resta TC, Gonzales RJ, Dail WG, Sanders TC, Walker BR (1997) Selective upregulation of arterial endothelial nitric oxide synthase in pulmonary hypertension. *Am J Physiol* 272: H806–H813.
47. Fike CD, Kaplowitz MR, Thomas CJ, Nelin LD (1998) Chronic hypoxia decreases nitric oxide production and endothelial nitric oxide synthase in newborn pig lungs. *Am J Physiol* 274: L517–L526.
48. Adnot S, Raffestin B, Eddahibi S, Braquet P, Chabrier PE (1991) Loss of endothelium-dependent relaxant activity in the pulmonary circulation of rats exposed to chronic hypoxia. *J Clin Invest* 87: 155–162.
49. Mam V, Tanbe AF, Vitali SH, Arons E, Christou HA, et al. (2010) Impaired vasoconstriction and nitric oxide-mediated relaxation in pulmonary arteries of hypoxia- and monocrotaline-induced pulmonary hypertensive rats. *J Pharmacol Exp Ther* 332: 455–462.
50. Morimura K, Yamamura H, Ohya S, Imaizumi Y (2006) Voltage-dependent Ca²⁺-channel block by openers of intermediate and small conductance Ca²⁺-activated K⁺ channels in urinary bladder smooth muscle cells. *J Pharmacol Sci* 100: 237–241.
51. Herrera GM, Pozo MJ, Zvara P, Petkov GV, Bond CT, et al. (2003) Urinary bladder instability induced by selective suppression of the murine small conductance calcium-activated potassium (SK3) channel. *J Physiol* 551: 893–903.
52. Littler CM, Wehling CA, Wick MJ, Fagan KA, Cool CD, et al. (2005) Divergent contractile and structural responses of the murine PKC-epsilon null pulmonary circulation to chronic hypoxia. *Am J Physiol Lung Cell Mol Physiol* 289: L1083–L1093.
53. Feletou M, Köhler R, Vanhoutte PM (2012) Nitric oxide: orchestrator of endothelium-dependent responses. *Ann Med* 44: 694–716.